PNAS
www.pnas.org

Supplementary Information for

Hurricanes fertilize mangrove forests in the Gulf of Mexico (Florida Everglades, USA)

Edward Castañeda-Moya[1], Victor H. Rivera-Monroy[2], Randolph M. Chambers[3], Xiaochen Zhao[2], Lukas Lamb-Wotton[4], Adrianna Gorsky[3], Evelyn E. Gaiser[1,4], Tiffany G. Troxler[1,4], John S. Kominoski[1,4], Matthew Hiatt[2, 5]

[1]Southeast Environmental Research Center, Institute of Environment, Florida International University, Miami, FL 33199; [2]Department of Oceanography and Coastal Sciences, College of the Coast and Environment, Louisiana State University, Baton Rouge, LA 70803; [3]W.M. Keck Environmental Field Laboratory, William & Mary, Williamsburg, VA 23187; [4]Department of Biological Sciences, Florida International University, Miami, FL 33199; [5]Coastal Studies Institute, Louisiana State University, Baton Rouge, LA 70803

***Corresponding Author*:** Edward Castañeda-Moya, Southeast Environmental Research Center, Institute of Environment, Florida International University, 11200 SW 8th St Bldg. OE 148, Miami, FL 33199, Phone: 305-348-7479, Email: ecastane@fiu.edu

www.pnas.org/cgi/doi/10.1073/pnas.1908597117

Supplementary Information Text

Methods

Study Sites. Mangrove wetlands in southwestern FCE encompass mixed-species stands of *Rhizophora mangle*, *Avicennia germinans*, *Laguncularia racemosa*, and *Conocarpus erectus*; the latter species is restricted to upstream locations of the estuary where salinity does not exceed 10 ppt (1-3). Mangrove areas in southeastern Florida are dominated by *R. mangle* scrub forests (tree height ≤1.5 m) with clusters of *C. erectus* and *L. racemosa* (e.g., TS/Ph-6 & 7) (2). Forests on the Ridge are dominated by *A. germinans* and *C. erectus*; whereas *R. mangle* occupies the fringe zone. Mangrove areas in southwestern FCE have a semi-diurnal tidal exchange (mean amplitude is 1.1 m) (4, 5). In contrast, mangrove areas in southeastern FCE ranged from non-tidal with flooded conditions (inland from the Ridge) to micro-tidal (Bay area) systems, but water flow and hydrologic connectivity with Florida Bay are determined by the interactions of seasonal precipitation, upland runoff, and wind (6, 7).

Sediment Deposition and Nutrient Inputs. To characterize storm sediment deposition with distance inland from shoreline, transects were established perpendicular to the shore at selected mangrove sites including SRS-5 (100 m), SRS-6 (350 m), WSC-9 (350 m), WSC-10 (350 m), WSC-13 (350 m), and Taylor Ridge (140 m). Within each river basin (Shark, Harney, Broad) transects were located in the middle and lower part of the estuary where most of hurricane impacts were evident (Figs. 4*A*, S1). In the Taylor River basin, the Ridge transect was located in the lower part of the estuary. At discrete mangrove sites (SRS-7, WSC-8, WSC-11, and WSC-12), soil-sediment cores were collected at 30-40 m from the forest edge. There was no evidence of storm deposition at SRS-4, WSC-7, and TS/Ph-6 & 7, and hence core sampling was not performed at these sites.

All soil-sediment samples were oven-dried at 60ºC to a constant weight and weighted to determine bulk density (grams of dried mass per cm^3 of wet soil). Core samples were ground with a Wiley Mill to pass through a 40-µm-mesh screen. OM content (% ashed-free dry weight) was determined by loss-on-ignition (LOI) at 550ºC for 4 h (8). TC and TN concentrations were determined for each sample with a NA1500 elemental analyzer (Fisons Instruments, Inc., Danvers, MA). Ashed samples were also analyzed for TIC and the percentage of organic carbon (C_{org}) was calculated as the difference between TIC and TC (9, 10). TP was extracted using an acid-digested (HCl) extraction and concentrations determined by colorimetric analysis (Methods 365.4 and 365.2, US EPA 1983). The Ca-bound inorganic P fraction was extracted from soil and sediment core samples with a 1 N HCl (11). After extraction, extracts were analyzed for soluble reactive P using the same protocol mentioned above. Carbon and nutrient (N and P) data were expressed on a volume basis using bulk density values.

For the transect data, we used a randomized block ANOVA design to test for differences in physico-chemical variables among sites, distance along transects, and layers (soil vs. sediment). All effects were considered fixed. Distance was nested within each site and treated as a block. Prior to analysis, the actual sampling distance along each transect was normalized on a scale from 0 to 1 to facilitate further ANOVA comparisons among main effects (12). Data collected within the discrete sites were analyzed separately with a two-way ANOVA to test for differences in physico-chemical variables among sites and layers. All pairwise comparisons were performed with Tukey's honestly significant difference (HSD). Variables were log-transformed (ln (x + 1); arcsine was used for organic matter) when required prior to analysis to meet the

ANOVA assumptions. Unless otherwise stated, data presented are the means (±1 SE) of untransformed data. Statistical analyses were performed with PROC MIXED (SAS Institute, Cary, NC, USA).

Long-term Soil Properties. Soil cores collected at each of the Shark River sites (SRS-4, SRS-5, and SRS-6) were processed separately in the laboratory. From each core, the fresh soils were homogenized, then a 1 cm^3 sub-sample was dried and weighed to determine bulk density. Organic matter content was determined by LOI. Total P was determined spectrophotometrically after acid (HCl) hydrolysis (13). Total C and N were determined on a Perkin-Elmer 2400 elemental analyzer. We used repeated measures ANOVA (PROC MIXED) to test for differences in bulk soil properties among sites and years, with year as the repeated measure.

Litterfall Collection and Nutrient Content. Mangrove litterfall dynamics have been monitored in all Shark River sites since January 2001 using the same collection method (2). Briefly, litterfall was collected monthly at all sites (10 baskets per site) using permanent 0.25 m^2 wooden baskets supported approximately 1.3 m above the soil surface and lined with 1 mm mesh screening. Litterfall from each basket was sorted, dried, and weighed by leaf species, reproductive parts by species, and woody material. Leaf litter data from three different years (2008, 2014, 2018) were selected from each site to identify species-specific foliar P responses post-Wilma's impact in 2005 and immediate post-Irma's impact in 2017. Foliar P content was determined in all samples using the same protocols mentioned above. We used an unbalanced factorial ANOVA to evaluate differences in foliar P content of brown-senescent leaves (leaf litter) among mangrove species and sites. All pairwise comparisons were performed with Tukey's honestly significant difference (HSD). Statistical analyses were performed with PROC MIXED (SAS Institute, Cary, NC, USA).

Landscape Total Phosphorus Loading Rates. We used data collected along transects and discrete sites to estimate TP loading rates in estuaries of the southwestern (Broad, Harney, Shark) FCE and the Taylor Ridge (Little Madeira Bay). Using the actual sediment deposition data measured along transects and their position along each estuary, we delimited a number of polygons to estimate total deposition per estuary (Fig. S8). The polygons were delineated following the contour of the estuary and the length of the transect; this length per estuarine region was considered the width of the polygons. For instance, in the case of the Broad River, we considered 30 m as the width of the deposition band/strip from the upstream site (WSC-11) to the midstream (WSC-12) location along the estuary (Fig. S8*A*). Since the length of the transect at WSC-13 was 350 m, we used this value as the width of the polygon and linearly traced the perimeter of the polygon down to the mouth of the estuary to delineate different sections; this procedure was repeated for both Harney (Fig. S8*B*) and Shark River (Fig. S8*C*) estuaries. Although in the case of Taylor Ridge we only sampled one transect (140 m), the boundaries of the polygon were extended laterally along the edge of the Ridge (Fig. S8*D*); this area was selected after an *in situ* visual inspection showing a homogenous distribution of storm surge deposition across the area. The total area per polygon was estimated using ArcGIS (ArcGIS Desktop 2010, ESRI Inc.). We only estimated the total deposition along the side of the estuary where actual field data were obtained. We considered these values conservative, first-rate estimates of this "new" TP input (opposite to regenerated *in situ*) into the mangrove wetlands at the landscape level. To determine if there were significant differences in TP concentrations

among transects and distances across all the estuaries, we performed a one-way ANOVA where the estuaries were considered the main factor, and each sampling point, the experimental unit regardless of location; this analysis was performed using JMP Pro 14 (SAS Institute, Cary, NC, USA).

Storm Surge Anomaly. A linear relationship was estimated as a proxy to characterize storm inundation and the magnitude of new sediment deposited in the mangrove forest as a result of the storm surge along the Shark, Harvey, and Broad River estuaries and in the Taylor Ridge region. We used hydrographs data from our mangrove sites to capture abrupt changes in water levels inside the forest and along main channels due to the storm surge (Fig. S7). One distinct characteristic of these hydrographs was a major drawdown in water level prior to the storm surge maximum and forest flooding, which we considered as an anomaly when compared to the typical tidal cycle in the region previous to the storm surge (Fig. S7). This phenomenon of receding waters along the coast below normal levels was due to the exceptionally low pressure at the center of the storm and strong offshore winds on the northern side of Irma's circulation (14). The water level difference between the antecedent drawdown and subsequent storm surge water level peak is henceforth referred to as the storm surge anomaly (SSA). A regression between SSA and the maximum sediment deposition depth was fitted using JMP Pro 14 to characterize the association between the magnitude of the TP deposition and flooding amplitude in conjunction with the relative energy throughout the study area.

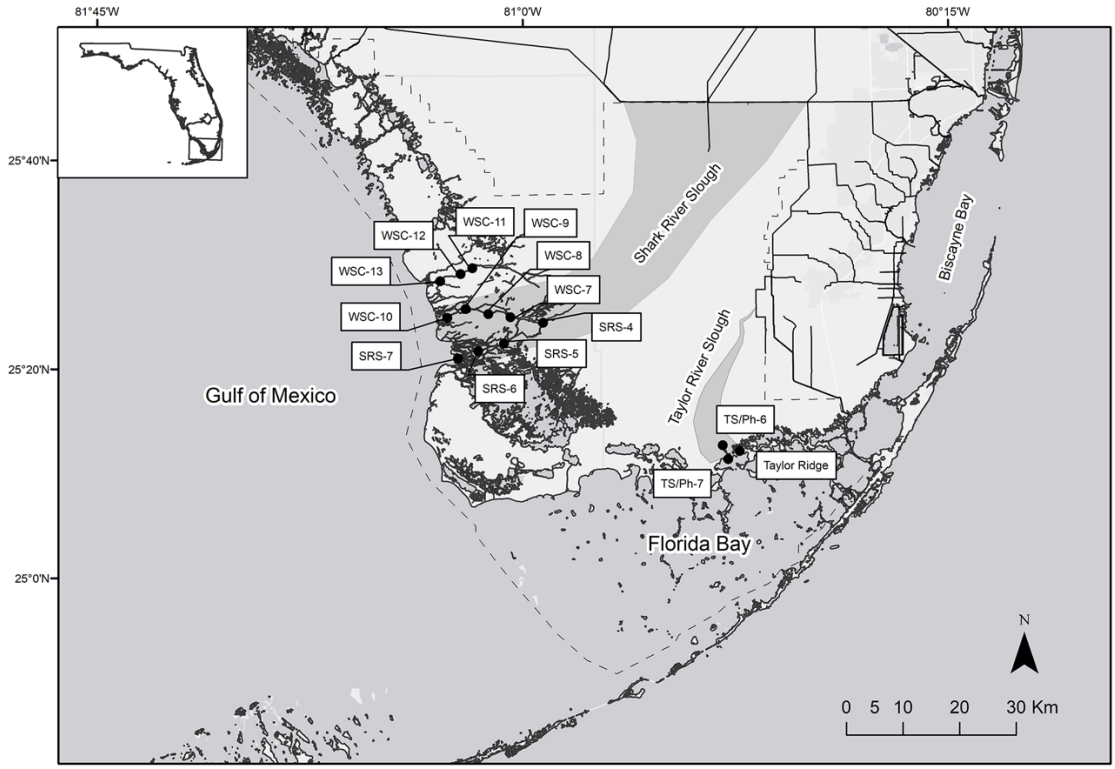

Fig. S1. Location of the study mangrove sites in the Florida Coastal Everglades (FCE), Everglades National Park (ENP) in south Florida, USA. SRS-4, SRS-5, SRS-6, and SRS-7 are located along Shark River estuary; WSC-7, WSC-8, WSC-9, and WSC-10 along Harney River estuary; WSC-11, WSC-12, and WSC-13 along Broad River estuary; TS/Ph 6 & 7 along Taylor River, and Taylor Ridge located ~1 km east from the mouth of Taylor River. The *insert* shows the location of ENP in south Florida, USA.

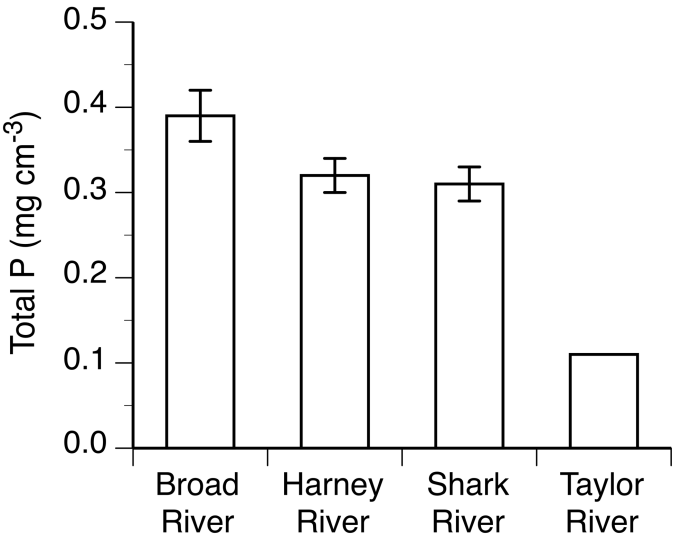

Fig. S2. Mean (± 1 SE) total phosphorus concentrations in storm-derived sediments at mangrove sites along estuaries in southwestern (Broad, Harney, and Shark Rivers) and southeastern (Taylor River) Florida Coastal Everglades after the passage of Hurricane Irma in September 10, 2017.

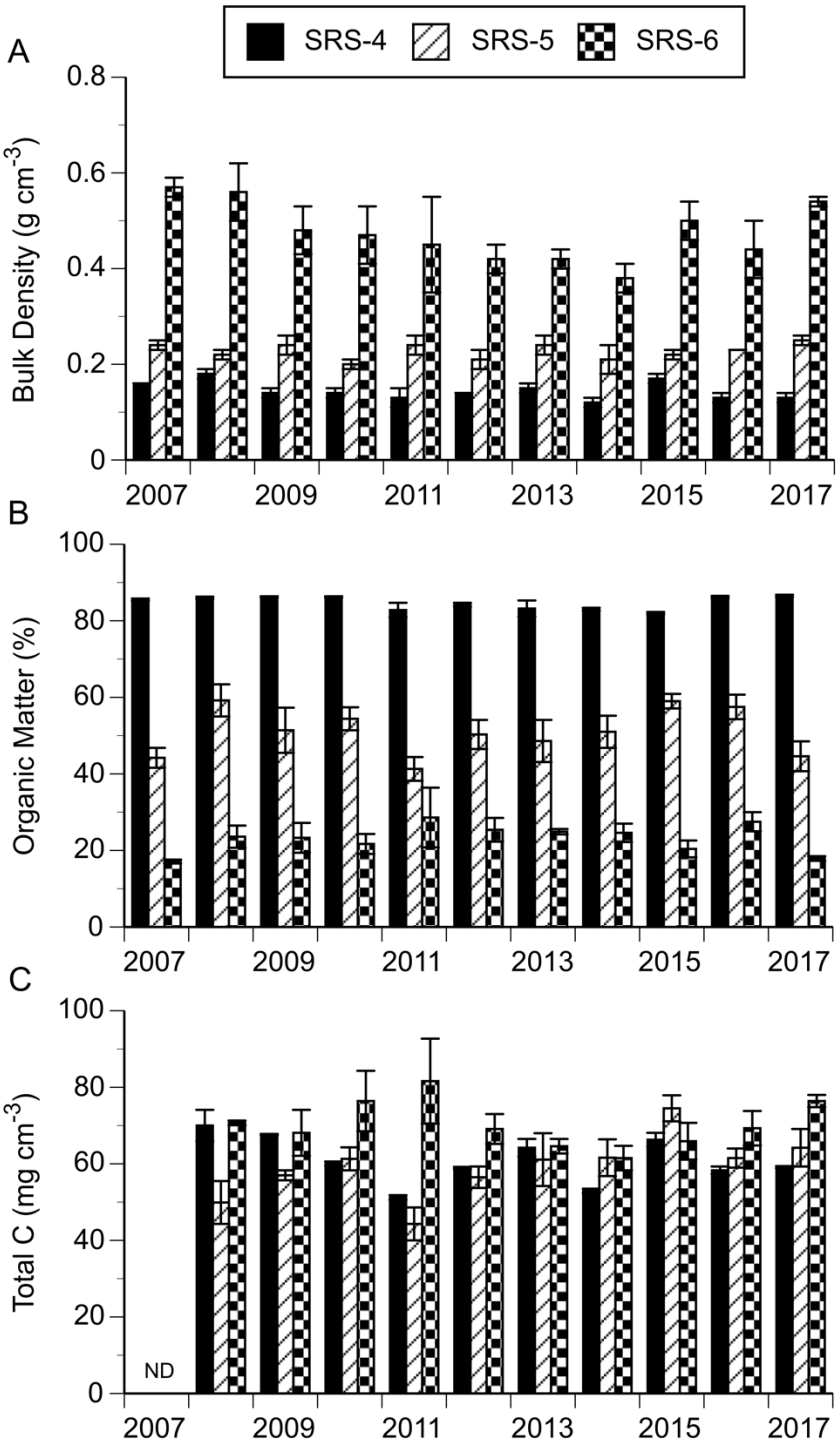

Fig. S3. Long-term variation in surface (top 10 cm) soil properties at mangrove sites along Shark River estuary in southwestern Everglades. *(A)* Bulk density. *(B)* Organic matter content. *(C)* Total carbon. Values represent the means ± 1 SE. ND indicates samples were not collected.

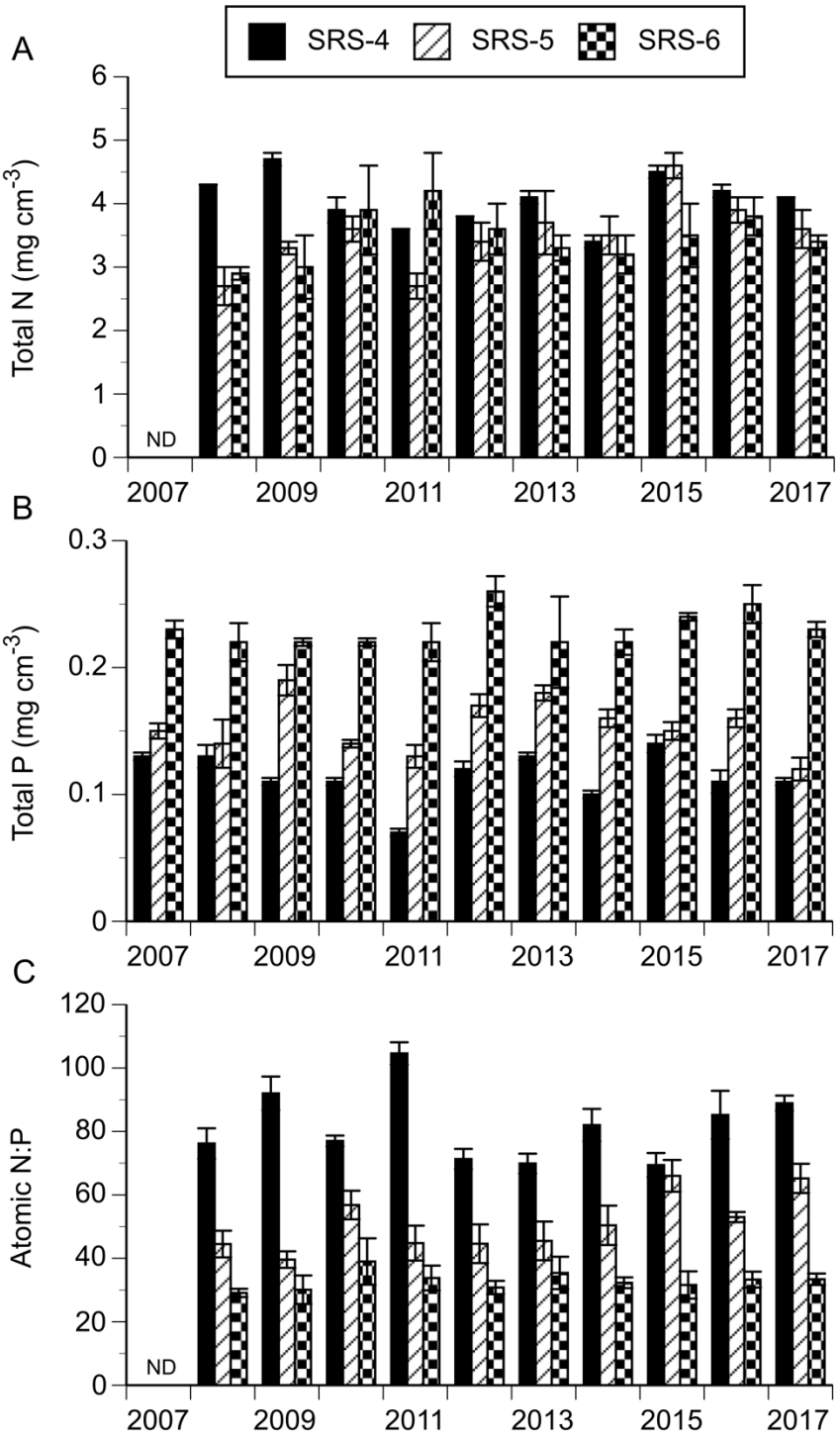

Fig. S4. Long-term variation in surface (top 10 cm) soil nutrient concentrations at Shark River mangrove sites in southwestern Everglades. *(A)* Total nitrogen. *(B)* Total phosphorus. *(C)* Atomic N:P ratio. Values represent the means ± 1 SE. ND indicates samples were not collected.

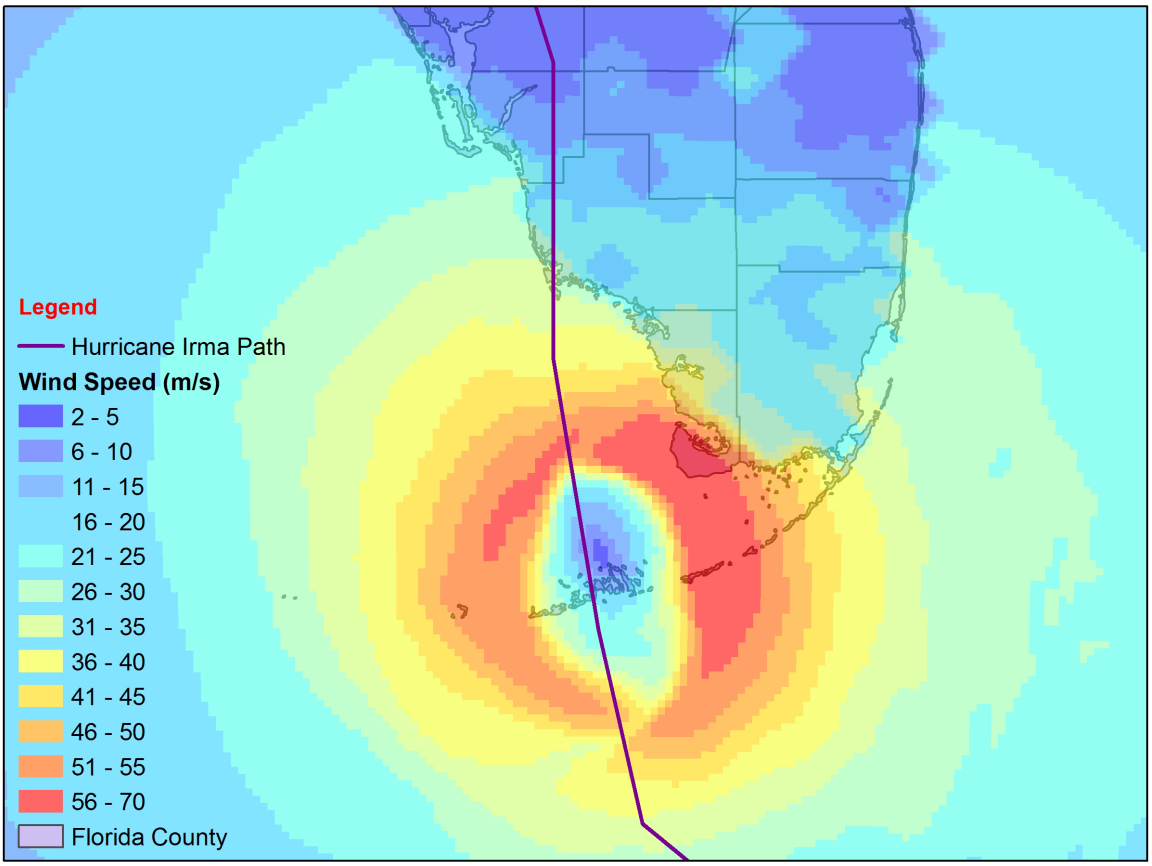

Fig. S5. Hurricane Ima's path and wind fields during its passage across south Florida. The wind speed represents maximum 1-min sustained surface wind 10 m above the ground/ocean surface. The wind field and track data were obtained from the Hurricane Research Division and the National Hurricane Center of the US National Oceanic and Atmospheric Administration.

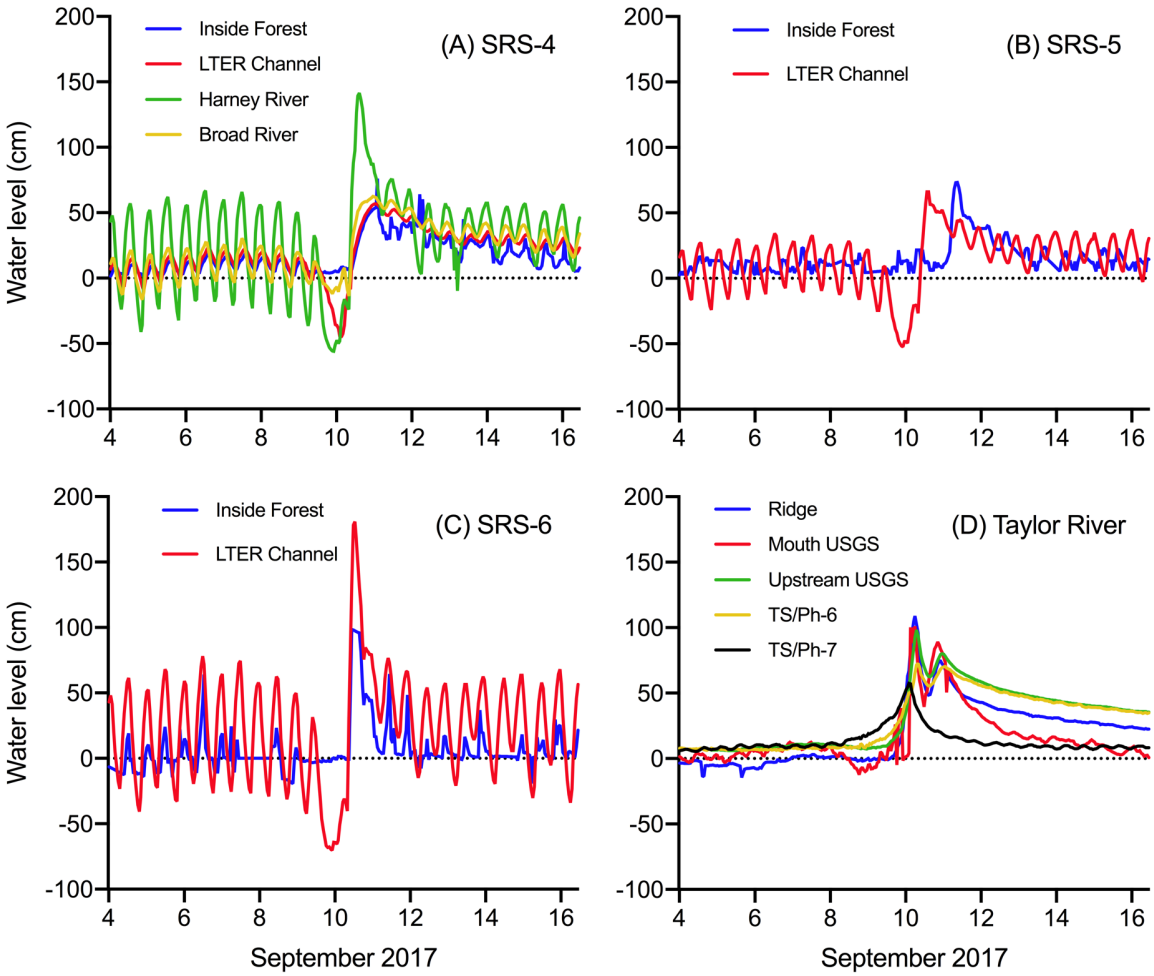

Fig. S6. Changes in water levels associated with Hurricane Irma's storm surge measured at FCE-LTER mangrove sites (channel and inside forest: SRS-4, SRS-5, SRS-6, TS/Ph-6, TS/Ph-7) and at channel gauges located in Broad, Harney, and Taylor (mouth USGS, Upstream USGS, Ridge) Rivers. The zero mark is relative to the soil surface at all mangrove sites and data are not referenced to the North American Vertical Datum of 1988 (NAVD88), except for Broad River in panel A.

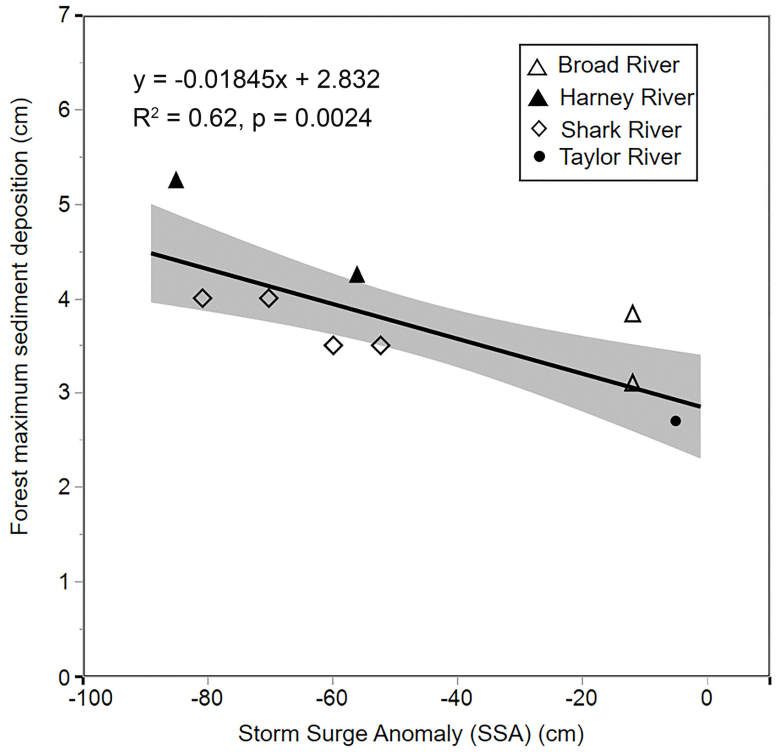

Fig. S7. Linear relationship between storm surge anomaly (SSA) and forest maximum sediment deposition depth. Standard parameters of the linear regression model are included.

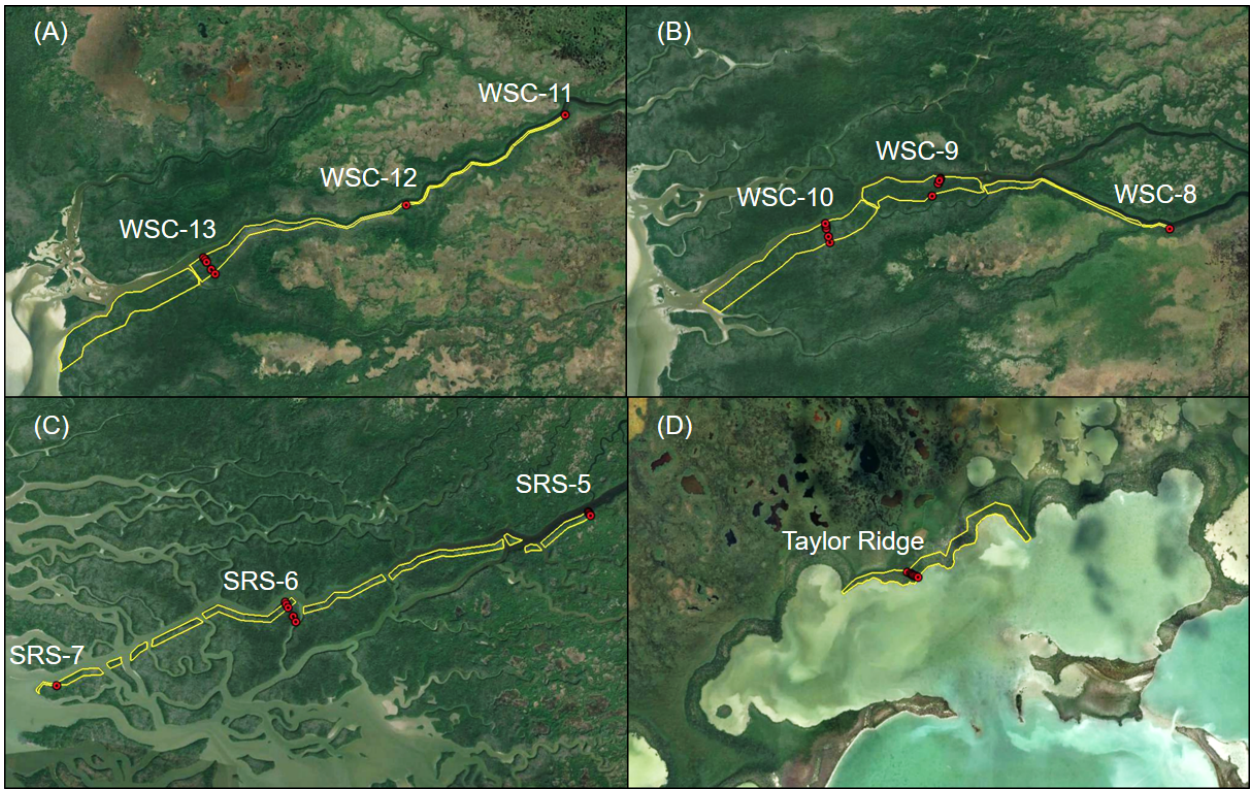

Fig. S8. Illustration of polygons delimited in mangroves sites to estimate total Irma's sediment deposition per estuary. The polygons were delineated following the contour of the estuary and the length of the transect and location of discrete sites; this length per estuarine region was considered the width of the polygons. *(A)* Broad River sites. *(B)* Harney River sites. *(C)* Shark River sites. *(D)* Taylor Ridge transect.

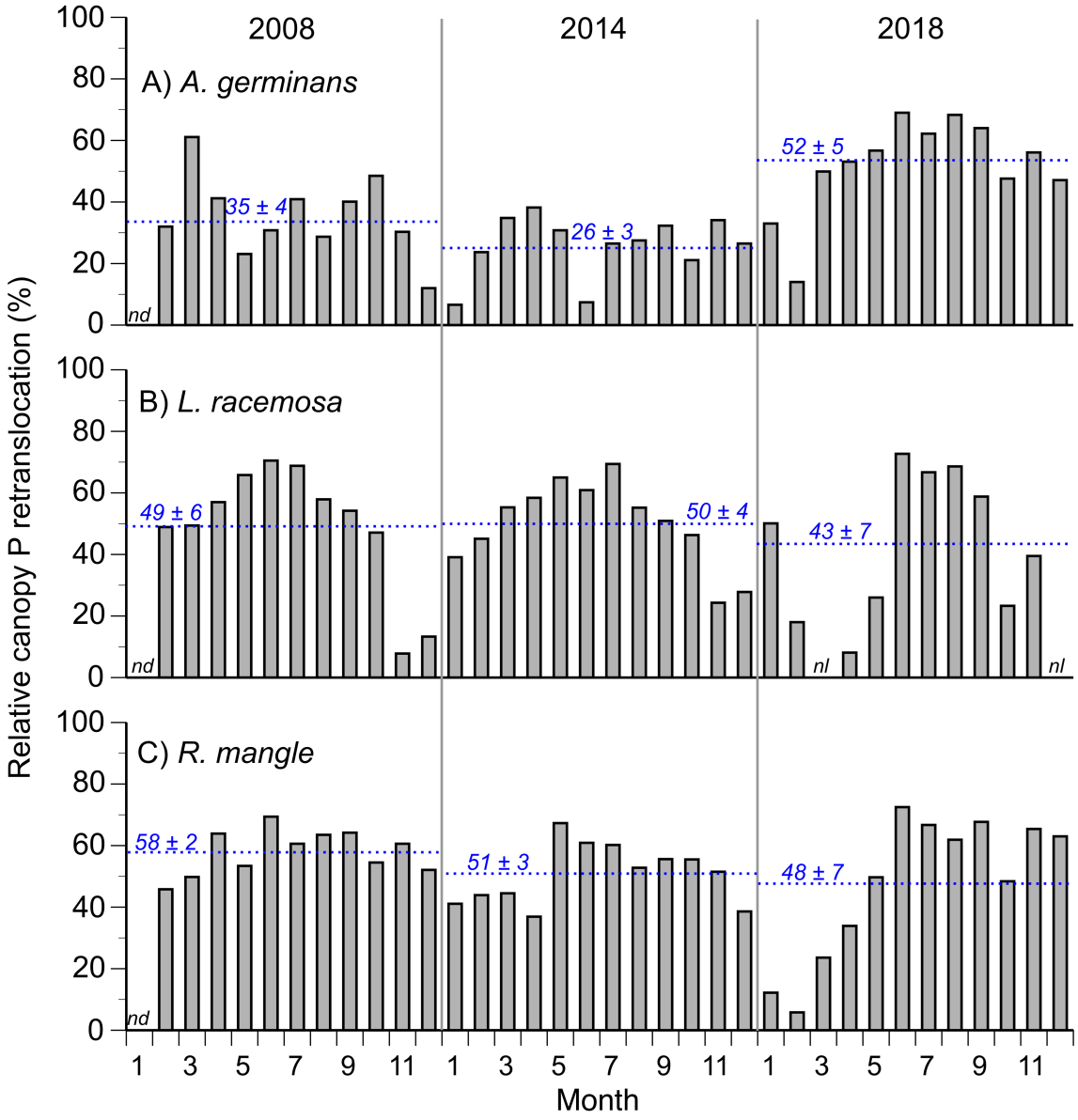

Fig. S9. Monthly relative canopy phosphorus (P) retranslocation efficiency of the mangrove species *Avicennia germinans*, *Laguncularia racemosa*, and *Rhizophora mangle* in SRS-6 during post-Wilma (2008 and 2014) and immediate post-Irma (2018) periods. Blue dotted lines represent mean (± 1 SE) annual values. nd = no data. nl = no leaf litter sample.

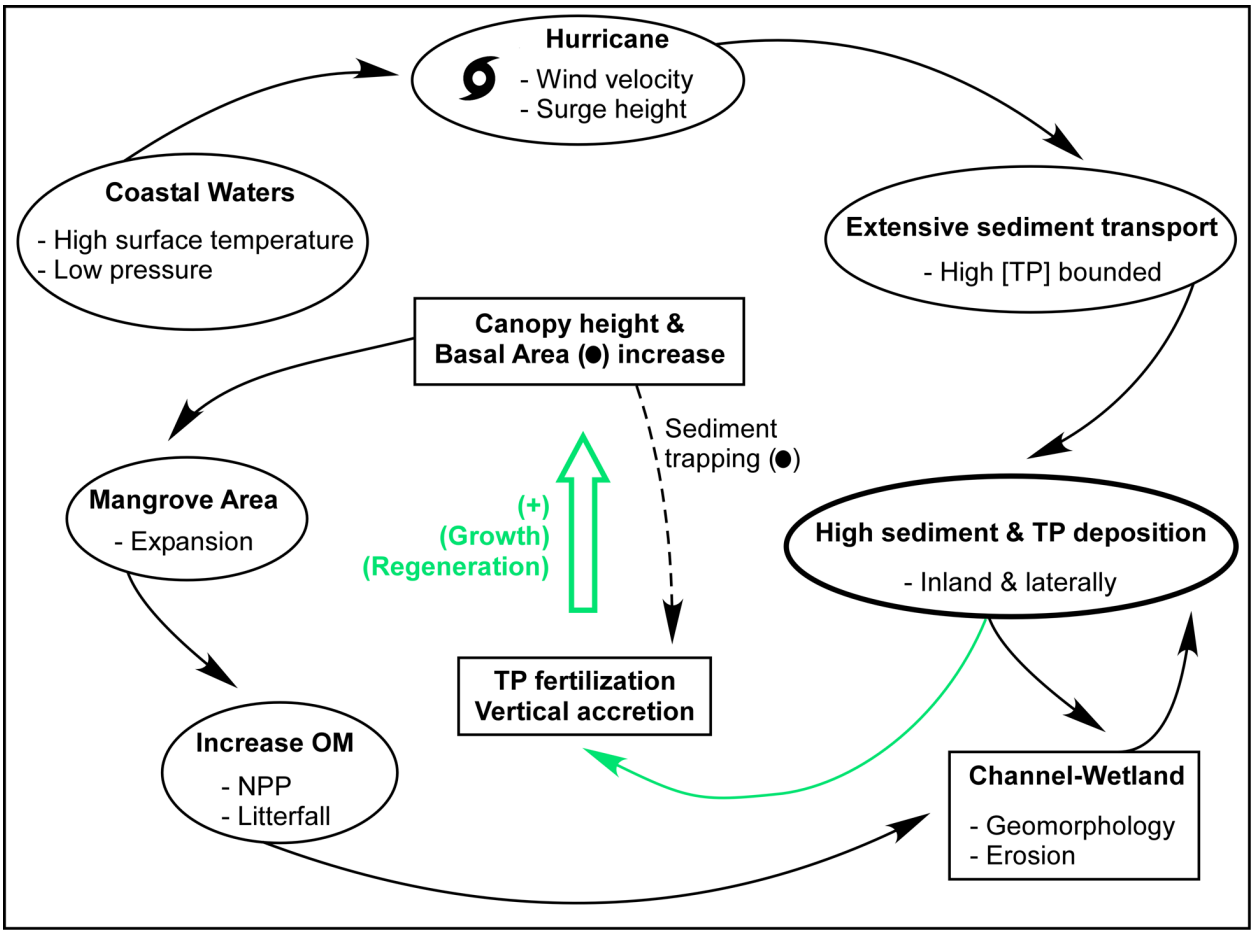

Fig. S10. Conceptual diagram showing positive (+ phosphorus fertilization, vertical accretion) hurricane influence interactions controlling mangrove wetland canopy height, primary productivity, and spatial distribution patterns as a result of hurricane disturbances in the Florida Coastal Everglades. The black dots in parenthesis indicate the influence of canopy height and basal area increase on sediment trapping. The dotted line arrow shows the indirect positive influence of canopy height and basal area increase on vertical accretion through sediment trapping.

Table S1. Statistical results of physico-chemical properties measured in storm sediments and surface soils (top 10 cm) along transects in mangrove sites of the Florida Coastal Everglades (FCE) after the passage of Hurricane Irma. Significance levels are indicated by * $P < 0.05$, ** $P < 0.01$, *** $P < 0.001$. ns = not significant. – = not determined

	Site			Distance (Site)			Layer (sediment vs. soil)			Site x Layer		
Variables	df [a]	F	p	df [a]	F	p	df [a]	F	p	df [a]	F	p
Deposition Depth (cm)	5, 31	108.7	***	25, 31	39.1	***	–	–	–	–	–	–
Bulk Density (g cm^{-3})	5, 87	102.5	***	25, 87	10.5	***	1, 87	163.7	***	5, 87	16.7	***
Organic Matter (%))	5, 87	22.1	***	25, 87	5.0	***	1, 87	221.7	***	5, 87	13.3	***
Total OC (mg cm^{-3})	5, 87	10.7	***	25, 87	3.4	***	1, 87	56.6	***	5, 87	1.6	ns
Total IC (mg cm^{-3})	5, 87	146.0	***	25, 87	10.9	***	1, 87	116.5	***	5, 87	15.3	***
Total N (mg cm^{-3})	5, 87	9.4	***	25, 87	3.5	***	1, 87	2.7	ns	5, 87	1.5	ns
Total P (mg cm^{-3})	5, 87	14.1	***	25, 87	2.9	***	1, 87	119.8	***	5, 87	33.4	***
Ca-bound P (mg cm^{-3})	5, 66	26.1	***	18, 66	6.1	***	1, 66	229.4	***	5, 66	19.4	***

[a] The degrees of freedom (df) of the denominator were adjusted with the Kenward-Roger method when required, SAS Proc Mixed.

Table S2. Physico-chemical properties of storm sediments and surface soils (top 10 cm) measured in transects at mangrove sites in the Florida Coastal Everglades (FCE) after the passage of Hurricane Irma. Means (± 1 SE) with different letters are significantly different (Tukey HSD post hoc test: $P < 0.05$) across sites and layers for each variable

Site	Bulk Density ($g\ cm^{-3}$)		Organic Matter (%)		Total OC ($mg\ cm^{-3}$)		Total IC ($mg\ cm^{-3}$)		Ca-bound P ($mg\ cm^{-3}$)	
	Storm sediments	Surface soils	Storm sediments	Surface soils	Storm sediments	Surface soils	Storm sediments	Surface soils	Storm sediments	Surface soils
SRS-5	0.47 ^{cd} (0.05)	0.13 ^{f} (0.01)	22.5 ^{c} (1.2)	62.6 ^{a} (5.5)	39.2 ^{ab} (3.8)	44.3 ^{a} (3.2)	25.7 ^{cd} (3.0)	0.8 ^{f} (0.3)	0.21 ^{ab} (0.03)	0.03 ^{e} (0.01)
SRS-6	0.44 ^{cd} (0.03)	0.20 ^{ef} (0.03)	19.2 ^{c} (0.6)	46.4 ^{b} (4.5)	28.0 ^{cd} (1.4)	38.8 ^{ab} (2.1)	26.9 ^{cd} (2.1)	5.6 ^{ef} (2.2)	0.19 ^{b} (0.01)	0.07 ^{cde} (0.01)
WSC-9	0.49 ^{bc} (0.04)	0.23 ^{ef} (0.05)	16.5 ^{c} (0.6)	48.9 ^{b} (7.5)	29.2 ^{cd} (1.6)	39.3 ^{a} (0.8)	33.1 ^{c} (3.0)	9.4 ^{ef} (4.2)	0.19 ^{b} (0.01)	0.06 ^{de} (0.02)
WSC-10	0.64 ^{b} (0.04)	0.34 ^{de} (0.08)	12.5 ^{c} (0.8)	38.1 ^{b} (6.6)	25.8 ^{d} (0.9)	35.5 ^{ab} (2.9)	48.2 ^{b} (4.6)	18.9 ^{de} (7.5)	0.22 ^{ab} (0.01)	0.12 ^{c} (0.02)
WSC-13	0.59 ^{bc} (0.06)	0.35 ^{de} (0.10)	19.0 ^{c} (1.8)	44.5 ^{b} (7.1)	30.2 ^{bcd} (1.5)	40.0 ^{a} (2.2)	39.9 ^{bc} (5.8)	17.2 ^{de} (9.2)	0.25 ^{a} (0.02)	0.11 ^{cd} (0.03)
Ridge	0.85 ^{a} (0.07)	0.96 ^{a} (0.05)	14.7 ^{c} (0.5)	14.4 ^{c} (0.8)	38.9 ^{a} (2.5)	42.2 ^{a} (2.6)	70.1 ^{a} (6.2)	80.8 ^{a} (4.4)	0.05 ^{e} (0.01)	0.08 ^{cde} (0.01)

Table S3. Physico-chemical properties of storm sediments and surface soils (top 10 cm) measured in discrete mangrove sites in the Florida Coastal Everglades (FCE) after the passage of Hurricane Irma. Means (± 1 SE) with different letters are significantly different (Tukey HSD post hoc test: $P < 0.05$) across sites and layers for each variable

Site	Bulk Density ($g\ cm^{-3}$)		Organic Matter (%)		Total OC ($mg\ cm^{-3}$)		Total IC ($mg\ cm^{-3}$)		Ca-bound P ($mg\ cm^{-3}$)	
	Storm sediments	Surface soils	Storm sediments	Surface soils	Storm sediments	Surface soils	Storm sediments	Surface soils	Storm sediments	Surface soils
SRS-7	0.63 [a]	0.33 [b]	11.7 [c]	24.6 [c]	26.6 [d]	37.7 [bc]	47.6 [a]	13.6 [c]	0.21 [abc]	0.13 [cd]
	(0.06)	(0.02)	(1.6)	(1.2)	(1.1)	(0.4)	(6.3)	(2.2)	(0.03)	(0.01)
WSC-8	0.52 [a]	0.18 [bc]	14.2 [c]	52.3 [b]	30.7 [cd]	44.0 [ab]	34.5 [ab]	3.2 [c]	0.19 [bc]	0.05 [de]
	(0.03)	(0.02)	(0.5)	(9.3)	(3.2)	(3.0)	(1.0)	(3.0)	(0.01)	(0.01)
WSC-11	0.54 [a]	0.14 [c]	21.1 [c]	77.3 [a]	32.4 [cd]	53.4 [a]	32.7 [b]	0.13 [c]	0.30 [a]	0.02 [e]
	(0.04)	(0.01)	(1.1)	(0.9)	(1.7)	(2.4)	(2.8)	(0.01)	(0.04)	(0.01)
WSC-12	0.58 [a]	0.15 [c]	19.3 [c]	64.4 [ab]	30.7 [cd]	47.5 [ab]	37.6 [ab]	0.17 [c]	0.28 [ab]	0.03 [de]
	(0.02)	(0.01)	(0.4)	(0.7)	(1.4)	(2.7)	(1.1)	(0.03)	(0.01)	(0.01)

Table S4. Total phosphorus (TP) loading rates in natural and constructed wetlands and managed agroecosystems. [*] Prescribed loading rates application before planting in mass per area

Country	Region	Habitat	Source	Dominant vegetation	TP loading rate (kg $ha^{-1}d^{-1}$)		
					Mean	Minimum	Maximum
USA	Broad River	Wetland	Hurricane sediment deposition	Mangrove	118.4	62.1	174.7
	Harney River				90.5	15.7	165.3
	Shark River				72.8	29.4	116.1
	Taylor River				18.5	7.8	29.1
USA	Upper Everglades; WCA-2A	Constructed Wetland (15)	Agriculture /Urban drainage	*Typha sp.*	0.019	0.011	0.031
				Typha sp. / Cladium jamaicense	0.008	0.001	0.017
				Cladium Jamaicense	0.004	0.002	0.007
USA	Everglades Nutrient Removal Project	Submerged Aquatic Vegetation Mesocosms (16)	Agricultural runoff	*Najas guadalupensis, Ceratophyllum demersum, Chara spp.*, *Potamogeton illinoensis*	0.297	0.123	0.226
USA	northern Everglades	Marshes and in field enclosures (17)	Agricultural discharges		0.011	0.022	0.351

Table S4 continued

Country	Region	Habitat	Source	Dominant vegetation	TP loading rate (kg ha^{-1}d^{-1})		
					Mean	Minimum	Maximum
USA	northern Everglade; WCA-2A	Stunted stands of sawgrass separated by shallow sloughs dominated by floating and attached cyanobacterial mats. (18)	Agricultural discharges		0.115	0.022	0.351
New Zeeland	Hamilton, Research farm	Constructed Wetland (19)	Dairy farm wastewater	*Schoenoplectus validus*	4.30	1.8	8.0
USA (Southeastern)		Constructed Wetland (20)	Free-floating plants	Mixed assemblage	5.5		
Australia, Canada, China, New Zealand, Poland, Sweden, The Netherlands, USA			Free water surface systems	Mixed assemblage	3.8		
Australia, Austria, Brazil, Canada, Czech Republic, Denmark, Germany, India, Mexico, New Zealand, Poland, Slovenia, Sweden, UK, US			Horizontal sub-surface flow	Mixed assemblage	3.9		
Australia, Austria, China, Denmark, France, Germany, Ireland, Poland, Norway, The Netherlands, Turkey, UK			Vertical sub-surface flow	Mixed assemblages	3.5		
USA		Agriculture Fields	Recommended fertilization	Corn (21-23)	104.2 [kg ha^{-1} days-cycle^{-1}]		
				Sugar Cane (24, 25)	94.4 [kg ha^{-1} days-cycle^{-1}]		
				Rice [*](26)		[56.0] kg ha^{-1}	[79.4] kg ha^{-1}

References

1. R. Chen, R. R. Twilley, Patterns of mangrove forest structure and soil nutrient dynamics along the Shark River Estuary, Florida. *Estuaries* **22**, 955-970 (1999b).
2. E. Castaneda-Moya, R. R. Twilley, V. H. Rivera-Monroy, Allocation of biomass and net primary productivity of mangrove forests along environmental gradients in the Florida Coastal Everglades, USA. *Forest Ecology and Management* **307**, 226-241 (2013).
3. J. L. Breithaupt, J. M. Smoak, C. J. Sanders, T. G. Troxler, Spatial variability of organic carbon, CaCO3 and nutrient burial rates spanning a mangrove productivity gradient in the coastal Everglades. *Ecosystems* 10.1007/s10021-018-0306-5 (2018).
4. M. W. Provost, Mean high water mark and use of tide-lands in Florida. *Florida Scientist* **36**, 50-66 (1973).
5. H. R. Wanless, R. W. Parkinson, L. P. Tedesco, "Sea level control on stability of Everglades wetlands" in Everglades. The ecosystem and its restoration S. M. Davis, J. C. Ogden, Eds. (St. Lucie Press, Delray Beach, Florida, 1994), pp. 199-223.
6. M. Sutula, J. W. Day, J. E. Cable, D. Rudnick, Hydrological and nutrient budgets of freshwater and estuarine wetlands of Taylor Slough in southern Everglades, Florida (U.S.A.). *Biogeochemistry* **56**, 287-310 (2001).
7. B. Michot, E. A. Meselhe, V. H. Rivera-Monroy, C. Coronado-Molina, R. R. Twilley, A tidal creek water budget: estimation of groundwater discharge and overland flow using hydrologic modeling in the southern Everglades. *Estuarine, Coastal and Shelf Science* **93**, 438-448 (2011).
8. B. E. Davies, Loss-on-ignition as an estimate of soil organic matter. *Soil Science Society of American Proceedings* **38**, 150-151 (1974).
9. W. E. Dean, Jr., Determination of carbonate and organic matter in calcareous sediments and sedimentary rocks by loss on ignition: comparison with other methods. *Journal of Sedimentary Petrology* **44**, 242-248 (1974).
10. J. W. Fourqurean, G. A. Kendrick, L. S. Collins, R. M. Chambers, M. A. Vanderklift, Carbon, nitrogen and phosphoris storage in subtropical seagrass meadows: examples from Florida Bay and Shark Bay. *Marine and Freshwater Research* **63**, 967-983 (2012).
11. M. J. Hedley, J. W. B. Stewart, B. S. Chauhan, Changes in inorganic and organic soil phosphorus fractions induced by cultivation practices and by laboratory incubations. *Soil Science Society of American Journal* **46**, 970-976 (1982).
12. E. Castaneda-Moya *et al.*, Sediment and nutrient deposition associated with Hurricane Wilma in mangroves of the Florida Coastal Everglades. *Estuaries and Coasts* **33**, 45-58 (2010).
13. R. M. Chambers, J. W. Fourqurean, Alternative criteria for assessing nutrient limitation of a wetland macrophyte (*Peltandra virginica* (L.) Knuth). *Aquatic Botany* **40**, 305-320 (1991).
14. NHC, Hurricane Irma. Tropical Cyclone Report. *National Hurricane Center*, 111p (2018).
15. G. B. Noe, D. L. Childers, R. D. Jones, Phosphorus biogeochemistry and the impact of phosphorus enrichment: Why is the Everglades so unique? *Ecosystems* **4**, 603-624 (2001).

16. F. Dierberg, T. DeBusk, S. Jackson, M. Chimney, K. Pietro, Submerged aquatic vegetation-based treatment wetlands for removing phosphorus from agricultural runoff: response to hydraulic and nutrient loading. *Water research* **36**, 1409-1422 (2002).
17. P. V. McCormick, J. A. Laing, Effects of increased phosphorus loading on dissolved oxygen in a subtropical wetland, the Florida Everglades. *Wetlands Ecology and Management* **11**, 199-216 (2003).
18. J. White, K. Reddy, Influence of nitrate and phosphorus loading on denitrifying enzyme activity in Everglades wetland soils. *Soil Science Society of America Journal* **63**, 1945-1954 (1999).
19. C. C. Tanner, J. S. Clayton, M. P. Upsdell, Effect of loading rate and planting on treatment of dairy farm wastewaters in constructed wetlands—II. Removal of nitrogen and phosphorus. *Water research* **29**, 27-34 (1995).
20. J. Vymazal, Removal of nutrients in various types of constructed wetlands. *Science of the total environment* **380**, 48-65 (2007).
21. W. M. Stewart, W. B. Gordon, Fertilizing for irrigated corn—Guide to Best management practices. International Plant Nutrition Institute. (2008).
22. AgSource-Laboratories, Phosphorus Recommendations. Technical Bulletin for Agronomy. F-16702-17. (2017).
23. R. D. Lee *et al.*, A guide to corn production in Georgia 2017. *College of Agriculture and Environmental Sciences* **Cooperative Extension Service. University of Georgia** (2017).
24. L. E. Baucum, R. W. Rice, An overview of Florida sugarcane. *Florida Cooperative Extension Service. University of Florida* **Pub. SS-AGR-232** (2009).
25. R. W. Rice, R. A. Gilbert, J. M. McCray, Nutritional requirements for Florida sugarcane. *Florida Cooperative Extension Service. University of Florida* **Pub. SS-AGR-228** (2018).
26. T. Roberts, N. Slaton, C. Wilson, R. Norman (2016) Soil Fertility. in *Arkansas rice production handbook MP192. Chapter 9* (Division of Agriculture, University of Arkansas, Little Rock, Arkansas).